

# **Acoustical Characteristics of Leak Signals in Plastic Water Distribution Pipes**

Paper published in *Applied Acoustics*, Volume 58 (1999), pp. 235-254

Osama Hunaidi and Wing T. Chu

National Research Council of Canada, Institute for Research in Construction

Ottawa, Canada K1A 0R6

(e-mail: [osama.hunaidi@nrc.ca](mailto:osama.hunaidi@nrc.ca) or [wing.chu@nrc.ca](mailto:wing.chu@nrc.ca))

# **Acoustical Characteristics of Leak Signals in Plastic Water Distribution Pipes**

Osama Hunaidi and Wing T. Chu

National Research Council Canada, Institute for Research in Construction  
Ottawa, Canada K1A 0R6

## **ABSTRACT**

Acoustical characteristics of leak signals in plastic pipes were investigated in this study for several types of leaks simulated under controlled conditions at an experimental site. The investigation included the characterization of frequency content of sound or vibration signals as function of leak type, flow rate, pipe pressure and season, the determination of the attenuation rate, and the variation of propagation velocity with frequency. The information presented in this paper for the acoustic characteristics of leak signals will help leak detection professionals in the selection of appropriate instrumentation, the design of appropriate measurement procedures, and in the case of propagation velocity, in accurately locating leaks using the cross-correlation method.

## INTRODUCTION

In many water distribution systems, a significant amount of water is lost due to leakage from distribution pipes. To reduce water loss, system operators conduct systematic programs to locate and repair leaks. Acoustic leak detection equipment is normally used to locate the leaks. Initially, listening rods and aquaphones are used to detect the sound induced by water leaks by placing them in direct contact with the pipes or their appurtenances, e.g., fire hydrants or control valves. Ground microphones are then used to pinpoint suspected leaks by listening for leak sounds on the pavement or soil directly above water pipes. Leak noise correlators, which are state-of-the-art computer-based devices, are also used to accurately pinpoint the location of suspected leaks. Several makes of acoustic leak detection equipment are commercially available.

The effectiveness of existing acoustic leak detection methods and equipment has been demonstrated extensively in the past, for example, by Fantozzi<sup>1</sup>, Fuchs<sup>2</sup>, and Liston<sup>3</sup>. Generally, acoustic methods are considered to be satisfactory by most users. This is only the case, however, where these methods are used for metallic pipes. For plastic pipes, the effectiveness of acoustic methods is not well established or documented. Most users are therefore skeptical about the accuracy of locating leaks in plastic pipes because problems that are normally encountered in locating leaks with acoustic equipment are more detrimental in the case of plastic pipes. These problems include interfering signals from road traffic or other sources, excessive signal attenuation, and insufficient sensitivity of instrumentation.

The lack of information regarding the effectiveness of acoustic leak detection methods for plastic pipes is alarming in view of the increasing world-wide use of these

pipes in water distribution systems. This has prompted a research project sponsored by the American Water Association Research Foundation (AWWARF) and the National Research Council Canada to evaluate the effectiveness of leak detection methods for plastic water distribution pipes. The project resulted in several findings and recommendations regarding measurement and analysis procedures to successfully locate leaks in plastic pipes<sup>4</sup>. In the part of the study presented in this paper, the acoustical characteristics of leak signals in plastic pipes were investigated. These included the frequency content of leak signals, attenuation rate, and variation of propagation velocity with frequency (or dispersion). Information about these characteristics is needed for the selection of appropriate instrumentation and measurement procedures, and in the case of propagation velocity, for the accurate determination of the location of leaks by the correlation method. Acoustical characteristics were determined in this study based on field tests at a specially constructed experimental leak detection facility.

## **TEST SITE AND MEASUREMENT PROCEDURE**

### **Leak Detection Site**

Tests were carried out at a leak detection facility at an experimental site located at the National Research Council (NRC) campus in Ottawa, Canada. The facility consisted of a 150 mm diameter PVC pipe that is about 200 m long. According to normal construction procedures, the pipe was buried in soft clay soil at a depth of 2.4 m. A plan view of the test facility is shown in Figure 1. Several types of leaks could be simulated at the experimental facility. As shown in Figure 2 (before back filling), the leaks included those from service connections, a faulty joint, and a cracked pipe (unfortunately, the cracked pipe collapsed soon after back filling). Leak rate and pipe pressure could be adjusted and measured to simulate various operational conditions. Leak-detection sensors, e.g., accelerometers or hydrophones, could be attached to various contact points with the test pipe including two fire hydrants that are about 100 m apart, as well as several 19 mm copper pipe service connections. The latter could also be used to simulate interfering noise induced by water consumption at residential connections.

### **Leak Sensors**

Both vibration and acoustic sensors were used to measure leak signals in the test pipe. For vibration measurement, piezoelectric accelerometers having a sensitivity of 1 volt/g were used. As shown in Figure 3, the accelerometers were attached magnetically to the top surface of fire hydrants while the latter were pressurized with water. For sound measurement, hydrophones having a sensitivity of 0.447 volts/kPa (44.7 volts/bar) were attached either to service connections as shown in Figure 4a or to fire hydrants through a

special pipefitting as shown in Figure 4b. The signals from the sensors were transmitted through 100 m long cables to the recording instrument.

### **Measurement Procedure**

Leak signals from the sensors were recorded simultaneously on a 16-bit digital tape recorder without conditioning for a duration of 5 minutes. Recorded signals were then played back off-site in analog form and re-acquired and analyzed using a PC-based data acquisition and analysis system. The signals were first passed through anti-aliasing filters with 200 Hz cut-off frequency. Then, a 66-second segment of each signal was digitized at a sampling frequency of 500 samples/second and stored on the hard disk of the PC. Spectral analysis was performed on the digitized signals using a 1024-point Fast Fourier Transform (FFT), Hanning window, and power-spectrum averaging. For computing the cross-correlation function via FFT, the digitized signals were band limited between 15 and 100 Hz using digital filtering. A rectangular 512-point force window with 50% overlap was also employed to eliminate the circular effect implicit in the discrete Fourier transform.

## RESULTS AND OBSERVATIONS

### Frequency Content

#### *Fire Hydrants versus Service Connections*

The frequency content of leak signals measured with hydrophones attached to 19 mm ( $\frac{3}{4}$  inch) copper service connections at the experimental leak facility was compared with that of hydrophones attached to fire hydrants. This was done in order to determine the suitability of signals measured at service connections for use in evaluating the attenuation characteristics of leak sounds. Frequency spectra are shown in Figure 5 for leak signals induced by a partially open underground service connection leak (see Figure 2c). The induced leak signals were measured simultaneously at the upstream fire hydrant and service connection No. 1 which are less than 1 m apart (see Figure 1). In spite of the close distance between the two measurement locations, it can be seen that the amplitudes at frequency components above 20 Hz at the service connection are significantly lower than those at the fire hydrant. Also there is an anomalous peak at about 90 Hz in the frequency spectrum of the leak signal at the service connection.

Initially, it was believed that the anomalous peak was dependent on the leak source – but as seen from Figure 6, this anomalous response was identical for different leak sources, e.g., petcock at nearby service connection No. 2 and faraway underground service connection leak. Apparently, the anomaly was due to the resonant response of the vertical service connection pipe.

Results obtained for leak signals measured at service connections were not reproducible. For example, when the hydrophone was removed and then attached again to a service connection, the above resonance peak occurred at a significantly different

frequency. The soil around the service connection was not well compacted and it seems that the coupling between the vertical service connection pipe and soil was easily changed. In view of this, leak signals were not measured any further in the study at service connections except for the evaluation of signal attenuation across pipe joints as there was no alternative.

### *Effect of Leak Type*

Frequency spectra of unfiltered leak signals and ambient noise (i.e. no leaks open) at the downstream fire hydrant are shown in Figure 7 for a joint leak and in Figure 8 for a service connection leak simulated by a partially open underground service connection. Spectra are shown for signals measured using both hydrophones and accelerometers. The following observations are based on these frequency spectra:

- There was no significant difference between the frequency content of signals induced by the joint and service connection leaks.
- Leak signals measured with hydrophones were significantly higher than ambient noise between 5 and 50 Hz. Below approximately 5 Hz, there was little difference between the leak signal and ambient noise although the amplitude was highest in this frequency range. It is believed that the signals below roughly 5 Hz are dominated by ambient noise at peaks corresponding to the longitudinal resonance frequencies of the test pipe. From theory, the first fundamental frequency should occur at about 1.25 Hz. The lowest frequency peak in Figures 7 and 8 agree with the theoretical value.

- Leak signals measured with accelerometers were not significantly higher than ambient noise. For frequencies up to about 50 Hz, leak signals were almost identical to ambient noise. Between 50 and 150 Hz, however, they were slightly higher than ambient noise. The higher frequency content for accelerometer signals in comparison with hydrophone signals is perhaps due to ground-borne ambient noise which unlike for hydrophones is readily picked up by accelerometers. These, however, were incoherent signals that did not affect the cross-correlation results significantly. The peaks or “spikes” seen in the frequency spectra of signals measured with both sensors could be attributed to several sources including longitudinal resonance of the water pipe, soil resonance, electrical noise caused by ground loops at the power mains frequency, or fundamental frequencies of rotating machinery, e.g., cooling tower fans (which was the case for the test site) or water pumps.

### *Effect of Pipe Pressure*

The frequency spectra of signals at the downstream fire hydrant (hydrant No. 2 in Figure 1) induced by the joint leak at pipe pressures of 137.9 and 413.7 kPa (20 and 60 psi) are shown in Figure 9. At low frequencies ( $\leq 35$  Hz), there was little difference between leak signals at low and high pressures. The higher pipe pressure, however, led to significantly greater amplitudes for high frequencies ( $\geq 35$  Hz). This is in qualitative agreement with the theoretical flow noise prediction that a higher pressure leads to higher flow rate for a fixed-size opening in the pipe and in turn leads to signals that have more high-frequency content<sup>5</sup>.

### *Effect of Leak Flow Rate*

For a particular pressure, the flow rate of the leak had a significant effect on the amplitude of measured signals, but had a negligible effect on their frequency content – i.e., the shape of the frequency spectra did not change. Frequency spectra of signals at the downstream fire hydrant induced by partially opening an underground service connection leak at flow rates of 3 and 7.5 *l/min* are shown in Figure 10. It can be seen that the high-flow rate leak led to signal levels that were almost 50 times those induced by the low-flow rate leak. This was true for most frequency components except those at the low end where ambient noise was dominant.

### *Effect of Season*

Seasonal effects on the frequency content of leak signals were significant. This can be seen from Figure 11 which shows the frequency spectra of signals at the downstream fire hydrant induced by the joint leak in both summer and winter. The depth of frozen soil in winter was not measured, but usually the frost penetration in Ottawa is roughly 1.5 m. At frequencies below 10 Hz, signals levels in winter were the same or slightly higher than those in summer. However, winter levels were lower than summer levels at higher frequencies. The lower levels in winter at high frequencies could be attributed to a higher attenuation rate in winter as mentioned further on. The higher winter attenuation rate is in agreement with the findings of an earlier study of ground-borne vibrations<sup>6</sup>. The shift from 65 to 55 Hz of a main frequency peak in the spectrum for the downstream hydrant is significant. The reason for this is unclear but as mentioned

earlier this could be due to a change in the coupling between the hydrant and soil as a result of freezing.

## **Attenuation Rate**

### *Along Pipe*

The attenuation rate of leak signals along the test pipe was evaluated by measuring leak signals at the upstream and downstream fire hydrants using hydrophones. Signals induced by the following two sources were measured: (i) joint leak which lies in the pipe segment bracketed by the hydrants provided an in-bracket source, and (ii) open valve at the most downstream point of the test pipe which lies outside the hydrants provided an out-of-bracket source. The net distance between the two receivers for the in-bracket source was 44.4 m and that for the out-of-bracket source was 102.6 m. The attenuation rate was determined from the transfer function between leak signals. The transfer function is an average of the ratio between two signals as a function of frequency. Transfer functions obtained for the two receiver-to-receiver distances are shown in Figure 9. The curves are “wavy” but they display the expected trend of greater attenuation for higher frequencies. Transfer functions obtained after smoothing with a 20-point moving average are shown in Figure 13. Smoothed transfer function values at selected frequencies are plotted in Figure 14 as a function of distance. Theoretically, all lines in Figure 14 should have a common origin but they are slightly off due to unknown factors. The gradient of each line is the attenuation rate for the corresponding frequency. The attenuation rate data points as a function of frequency are shown in Figure 15. Based

on these results, an overall attenuation rate was roughly estimated at 0.25 dB/m, i.e. 3% amplitude loss per meter.

Attenuation measurements in the winter were difficult to perform because of the low signal amplitude as can be seen in Figure 11 which shows frequency spectra of signals at the downstream fire hydrant induced by the joint leak in summer and winter. The smoothed transfer functions obtained with the same measurement technique and leak sources used in the summer investigation show useful data only in a fairly limited frequency range (10-20 Hz) as indicated in Figure 16. Based on the results at 15 Hz, an attenuation rate of 0.33dB/m was estimated which is significantly higher than the corresponding summer rate.

#### *Across Joints*

The attenuation rate of leak signals across a joint in the test pipe was evaluated from leak signals measured with hydrophones at service connections Nos. 3 and 4 (see Figure 1). These two service connections bracketed a pipe joint and were about 1 m apart. Therefore, the transfer function between leak signals measured at these points provided a direct indication of signal attenuation across the joint. Signals induced by the following two sources were measured: (i) partially open underground service connection leak which induced leak signals travelling upstream, and (ii) petcock at service connection No. 2 which induced leak signals travelling downstream. One source would have been sufficient, but two different sources were used as a check on accuracy. The sensitivities of hydrophones were not necessarily identical (manufacturer's specified sensitivity was within  $\pm 3$  dB as for most makes). In order to determine the difference between

hydrophone sensitivities, leak signals induced by the downstream source were measured with the sensors in a certain order and then measured again with the sensors in the reverse order. The resulting transfer functions are shown in Figure 17. There was a 1.3 dB difference between the hydrophone sensitivities. This was used to correct the transfer functions between hydrophone signals.

Corrected transfer functions obtained with the upstream and downstream sources are shown in Figure 18. At high frequencies, the transfer function values obtained with the downstream source are influenced by the resonance of the service connection pipe, and hence are ignored. For frequencies up to about 40 Hz, transfer function values obtained with both signal sources are very close to zero. Therefore, it was concluded that the attenuation of leak signals across pipe joints was insignificant.

## **Propagation Velocity**

### *Calculation Methods*

Propagation velocity of broad-band leak signals in water pipes could be easily calculated by using either the “time-of-flight” method or the cross-correlation method. In the time-of-flight method, the propagation velocity is estimated based on the difference in arrival times of transient signals measured at two locations that are a known distance apart. Velocity is then calculated as the distance traveled divided by the difference in arrival times. At the experimental facility utilized in this study, transient signals were generated in the test pipe by abruptly opening and then closing valves either at the most down stream point of the test pipe (out-of-bracket source) or at service connection No. 6 (in-bracket source). Typical measured transient signals are shown in Figure 19.

In the cross-correlation method, the propagation velocity is estimated based on the time lag between coherent continuous signals measured at two points that are a known distance apart. The signals are generated using a source at a known location. The velocity is then calculated based on the net traveled distance of measured signals and the time shift. At the experimental facility, signals were induced in the pipe by using either the joint leak or by opening the valve at the down stream end of the pipe.

### *Effect of Signal Source*

The effect of signal source was more important for the cross-correlation method than for the time-of-flight method. This could be explained as follows. The cross-correlation method is based on the similarity between measured signals which is affected by dispersion and frequency-dependent attenuation among other factors. Therefore, the shorter the net distance between measurement points, the more similar the signals and hence the more relevant their cross-correlation. The net distance for in-bracket sources is always shorter than that for out-of-bracket ones.

Cross-correlation functions obtained for both types of sources are shown in Figure 20. It is clearly seen that the cross-correlation peak for the out-of-bracket source is less definite than that for the in-bracket source. The almost sinusoidal shape of cross-correlation function obtained with the out-of-bracket source is indicative of the narrow-bandedness of measured signals as a result of their attenuation over a long propagation distance. Calculated velocities were 482 and 466 m/s for the in-bracket and out-of-bracket sources, respectively.

On the other hand, propagation velocities calculated by the time-of-flight method with the in-bracket and out of bracket sources were similar – velocities were 506 and 503 m/s, respectively. These values were slightly higher than those obtained with the cross-correlation of continuous signals. However, with the exception of the velocity calculated by the cross-correlation method with the out-of-bracket source, the slight difference in velocities calculated by the two methods had insignificant effect on the accuracy of leak location.

#### *Effect of Sensor Type*

Velocities determined for signals measured with hydrophones were not significantly different from those determined for signals measured with accelerometers. Slightly different time delays were obtained from the cross-correlation of either hydrophone or accelerometer signals – calculated velocities were 482 m/s and 492 m/s, respectively. Many leak detection practitioners are surprised at this due to the common belief that vibration signals propagate in the pipe wall whereas sound signals propagate in the water core and hence their velocities would be different. Obviously, this is not the case. Wave propagation in fluid-filled pipes is a complicated phenomenon. In simple terms, however, waves do not propagate separately in the water core and pipe wall – rather, propagation modes in both media are coupled. That is why the propagation velocity depends on the diameter and stiffness of the pipe material among other factors. According to this explanation also, the attenuation rate is believed to be the same for so-called “water-core” and “pipe-wall” transmitted vibration. The main attenuation mechanism in water-filled pipe is the radiation of energy into the surrounding soil as the

pipe wall vibrates, e.g., expands and contracts. This explains why plastic pipes have higher attenuation than metallic ones since the former are more flexible and hence are more effective energy radiators.

### *Effect of Frequency*

The Propagation velocity as a function of frequency was determined from the unwrapped relative phase angle of the transfer function using the relationship

$$V = 360 D f / \theta$$

where  $D$  is the net traveled distance,  $\theta$  is the unwrapped phase angle in degrees,  $f$  is the frequency in Hz, and  $V$  is the wave velocity. The phase angle is usually calculated and displayed in the range  $\pm 180^\circ$  and hence is wrapped. The unwrapped phase angle is determined by adding an appropriate number of 360-degree cycles to the wrapped relative phase angles. The relative phase angle spectrum obtained from signals induced by the joint leak is shown in Figure 21. Even though the phase angle spectrum looks irregular, most likely due to out-of-bracket background noise and reflections, satisfactory results were obtained. Results are shown here for frequencies whose relative phase angles were zero as marked on the spectrum in Figure 21. Corresponding unwrapped phase angles at these frequencies are shown in Figure 22. These points fall almost on a straight line passing through the origin – thus indicating that propagation velocity is independent of frequency. Based on the slope of the best-fit line in Figure 22, a velocity of 488 m/s was determined which is in close agreement with velocities obtained by the cross-correlation and time-of-flight methods.

### *Effect of Pipe Pressure*

Propagation velocities in the test pipe did not change significantly with pressure. Average velocity values measured using the time-of-flight method for an out-of-bracket source were 498 m/s and 504 at pipe pressures of 172.4 and 413.7 kPa (25 and 60 psi), respectively.

### *Effect of Season*

There was a minor difference in propagation velocities measured during summer and winter. The propagation velocity calculated by using the cross-correlation method and the joint leak as an in-bracket source was 515 m/s during winter in comparison with 482 m/s during summer – a difference of 7%. The measured water temperature was 16<sup>0</sup> C in the summer and 8<sup>0</sup> C in the winter. The higher velocity in winter is most likely due to a higher stiffness of the pipe wall and perhaps an increase in the density of the water core as a result of lower water temperature in winter.

## SUMMARY

The characteristics of leak signals in a typical PVC water distribution pipe have been investigated under controlled conditions at an experimental leak detection facility. The main findings of the investigation can be summarized as follows:

- Most of the frequency content of leak signals measured with hydrophones was below 50 Hz. Signal amplitudes at higher frequencies were extremely small. Accelerometer measured leak signals had higher levels at high frequency than hydrophone measured leak signals.
- The amplitude of leak signals diminished rapidly with distance, at a rate of about 0.25 dB/m. The winter's rate is significantly higher.
- Below 50 Hz, there was no measurable attenuation across pipe joints.
- The propagation velocity of leak signals is identical for both hydrophone and accelerometer-measured signals. The propagation velocity was about 7% higher in winter.
- Below 50 Hz, the propagation velocity is independent of frequency.

## **ACKNOWLEDGEMENT**

The work presented in this paper was part of a research project on leak detection methods for plastic water distribution pipes. The project was carried out with joint funding by the American Water Works Association Research Foundation and the National Research Council of Canada, and with in-kind support from the Regional Municipality of Ottawa-Carleton and the Louisville Water Company.

## REFERENCES

- 1 Fantozzi, M., G. Di Chirico, E. Fontana, and F. Tonolini, Leak Inspection on Water Pipelines by Acoustic Emission with Cross-Correlation Method. *Annual Conference Proceeding, American Water Works Association, Engineering and Operations*, 1993, 609-621.
- 2 Fuchs, H.V. and R. Riehle, Ten Years of Experience with Leak Detection by Acoustic Signal Analysis. *Applied Acoustics*, 1991, **33** (1), 1-19.
- 3 Liston, David A. and James D. Liston. Leak Detection Techniques. *Journal of the New England Water Works Association*, 1992, **106** (2), 103-108.
- 4 Hunaidi, O., W.T. Chu, A. Wang and W. Guan, Effectiveness of leak detection methods for plastic water distribution pipes. *Workshop on Advancing the State of our Distribution Systems- The Practical Benefits of Research, American Water Works Association Distribution System Symposium, Austin, Texas*, 1998, 1-8.
- 5 Beranek, L.L., and I.L. Ver, *Noise and Vibration Control Engineering – Principles and Applications*. John Wiley & Sons, Inc., New York, 1992.
- 6 Hunaidi, O., P.A. Chen, J.H. Rainer and M. Tremblay, Shear Moduli and Damping in Frozen and Unfrozen Clay by Resonant Column Tests. *Canadian Geotechnical Journal*, 1996 33 (3): 510-514.

## Figures Caption

- Fig.1 Plan view of the experimental leak detection facility.
- Fig. 2 Simulated leak types : (a) cracked pipe, (b) faulty joint, (c) service connection.
- Fig.3 Attachment of accelerometers to fire hydrant
- Fig.4 Attachment of hydrophones: (a) to service connection pipe, and (b) to fire hydrant
- Fig.5 Frequency spectra of leak signals at the upstream fire hydrant and nearby service connection No.1 induced by a 0.64 cm (1/4") underground nozzle leak.
- Fig.6 Frequency spectra of leak signals at service connection No.1 induced by open petcock at service connection No.2 and 0.64 cm (1/4") underground nozzle leak.
- Fig.7 Comparison of frequency spectra of joint leak and ambient noise measured by two different sensors. (a) hydrophone, (b) accelerometer.
- Fig.8 Comparison of frequency spectra of signals, induced by partially-open 0.64 cm (1/4") underground nozzle and ambient noise, measured by two different sensors. (a) hydrophone, (b) accelerometer.
- Fig.9 Frequency spectrum of leak signals induced by fully open joint leak at pipe pressures of 137.9 and 413.7 kPa (20 and 60 psi).
- Fig.10 Frequency spectrum of signals induced by 0.64 cm (1/4") underground nozzle open at flow rates of 3 and 7.5 *l/min*.
- Fig.11 Frequency spectrum of joint leak signals measured in summer and winter.
- Fig.12 Transfer functions obtained with the joint leak and an open valve at the downstream end of the NRC test pipe for signals measured at the upstream and downstream hydrants.
- Fig.13 Smoothed transfer functions of Fig.9.

- Fig.14 Transfer function at various frequencies versus net propagation distance.
- Fig.15 Attenuation rate as a function of frequency based on data in Figure 11.
- Fig.16 Smoothed transfer functions obtained with the joint leak and an open valve at the most downstream point of the NRC test pipe for signals measured at the upstream and downstream hydrants in winter.
- Fig.17 Comparison of transfer functions between leak signals across a pipe joint measured with hydrophone pairs arranged in opposite orders to determine error due to variation in sensitivity between sensors (0.64 cm underground nozzle used as leak source).
- Fig.18 Transfer functions between leak signals across a pipe joint obtained with upstream leak at service connection No.2 and downstream leak at the 0.64 cm underground nozzle. Transfer functions were compensated for variation in sensitivity between sensors.
- Fig.19 Typical transient hydrophone signals induced by abruptly opening and then closing a 2.54 cm (1") valve at the most downstream point of the NRC test pipe.
- Fig.20 Comparison of cross-correlation of signals induced by different sources.  
(a) the joint leak (in-bracket source), (b) the 2.54 cm valve at the most downstream point of the NRC test pipe (out-of-bracket source).
- Fig.21 Relative phase angle spectrum between acceleration leak signals at the upstream and downstream hydrants induced by the joint leak.
- Fig.22 Unwrapped relative phase angles and a best-fit line for selected frequencies.





(a)



(b)



(c)

Figure 2

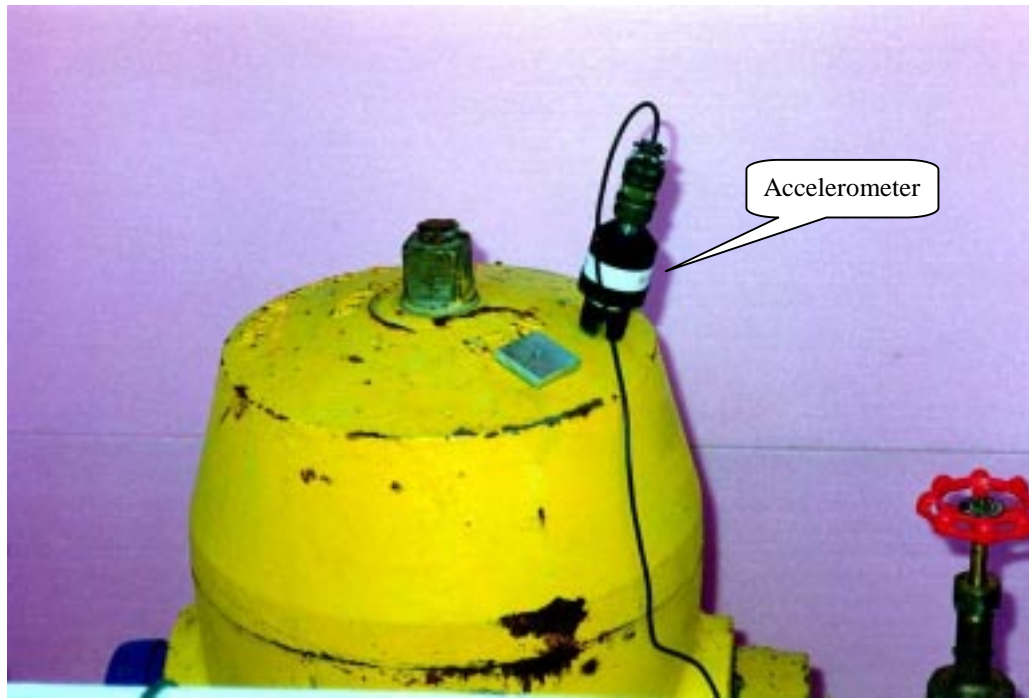


Figure 3



(a)



(b)

Figure 4

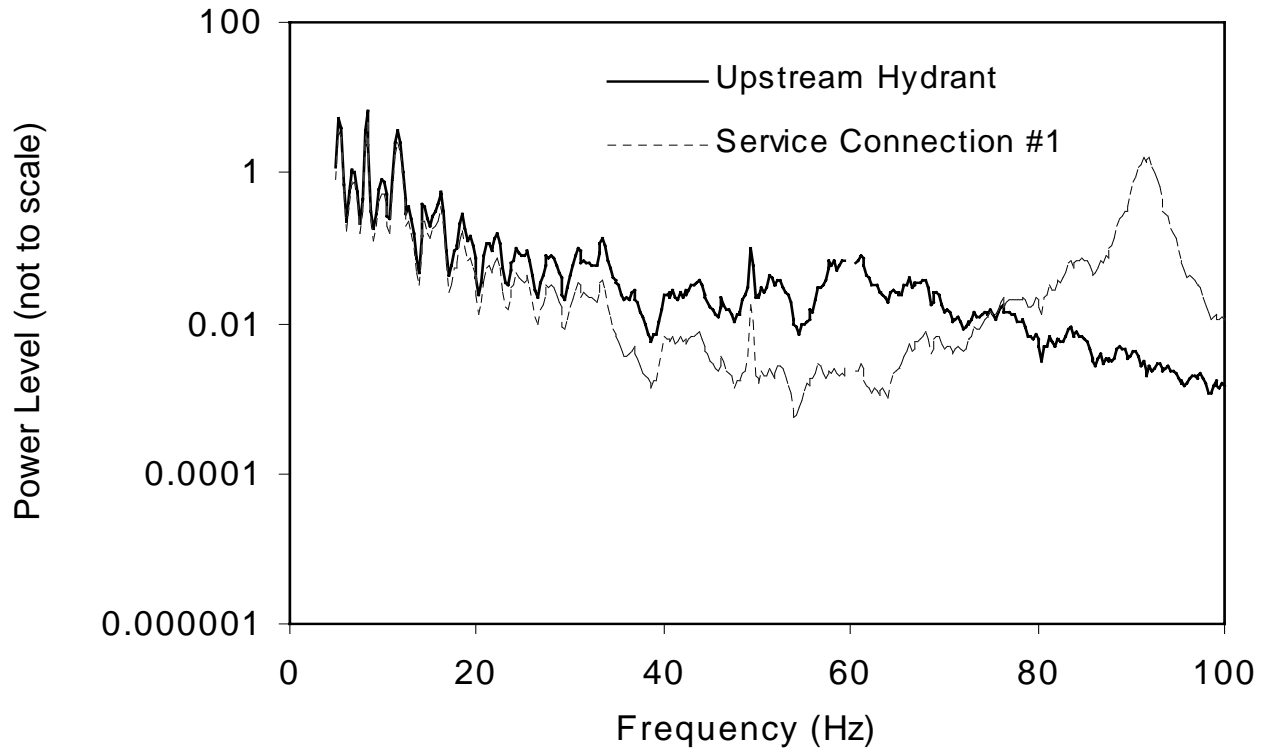


Figure 5

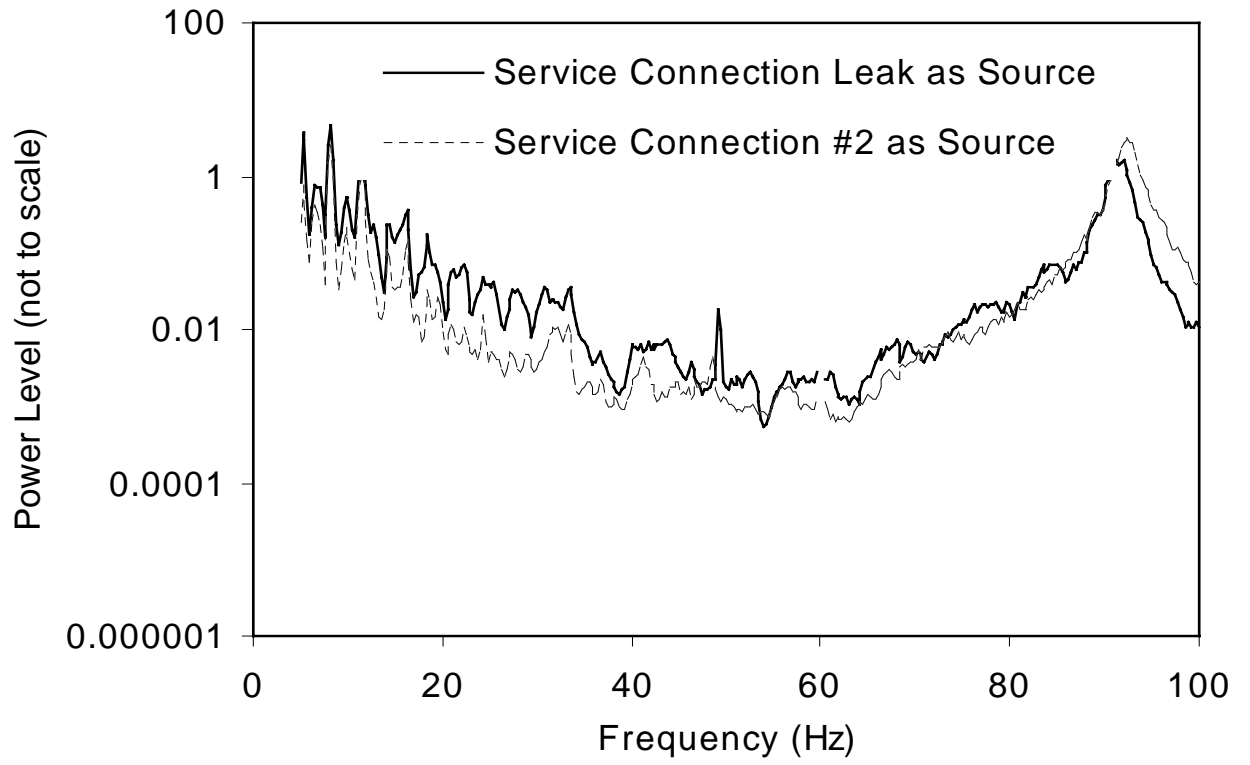


Figure 6

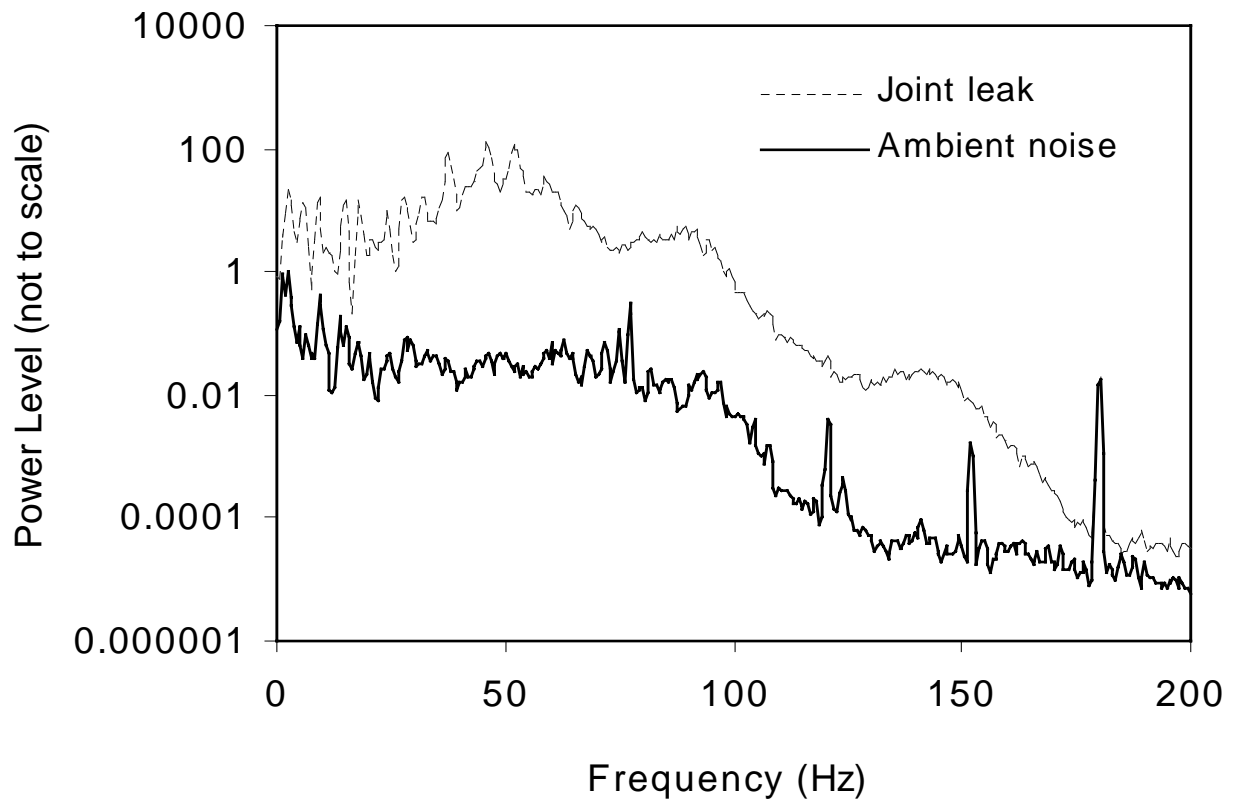


Figure 7a

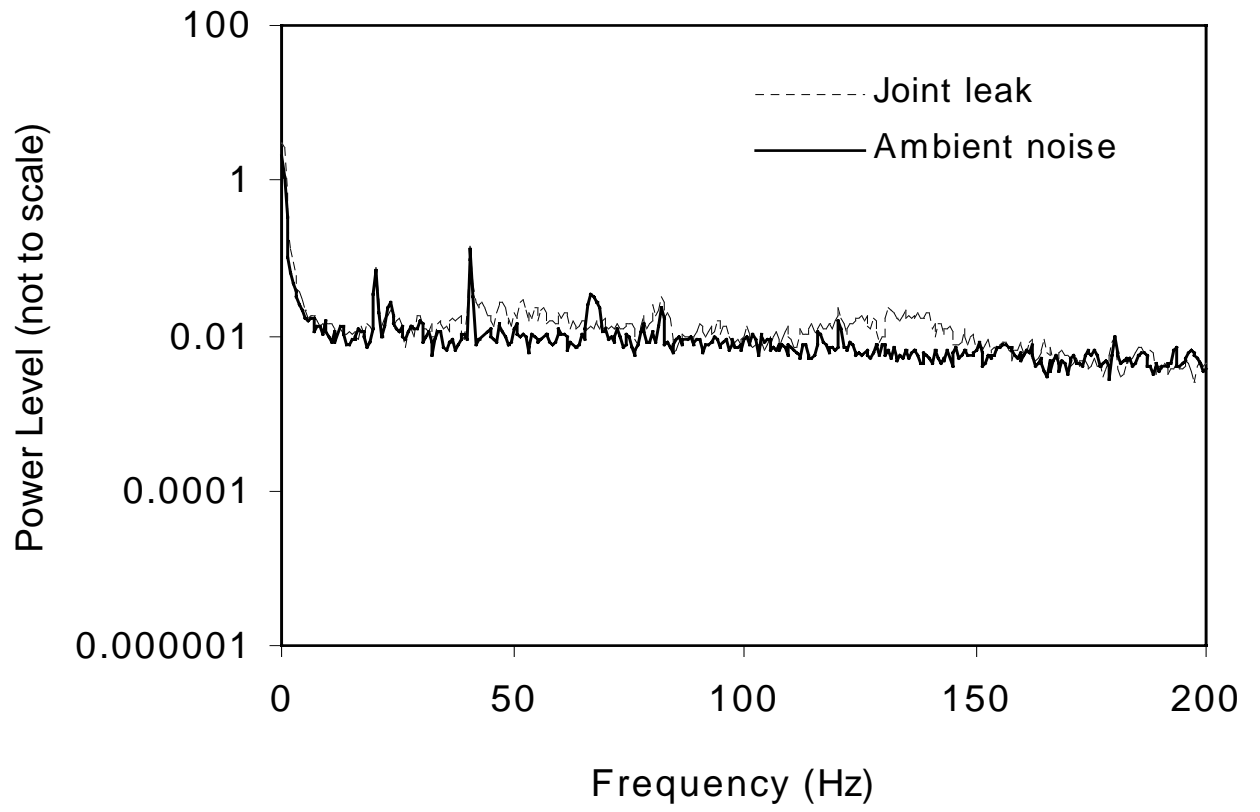


Figure 7b

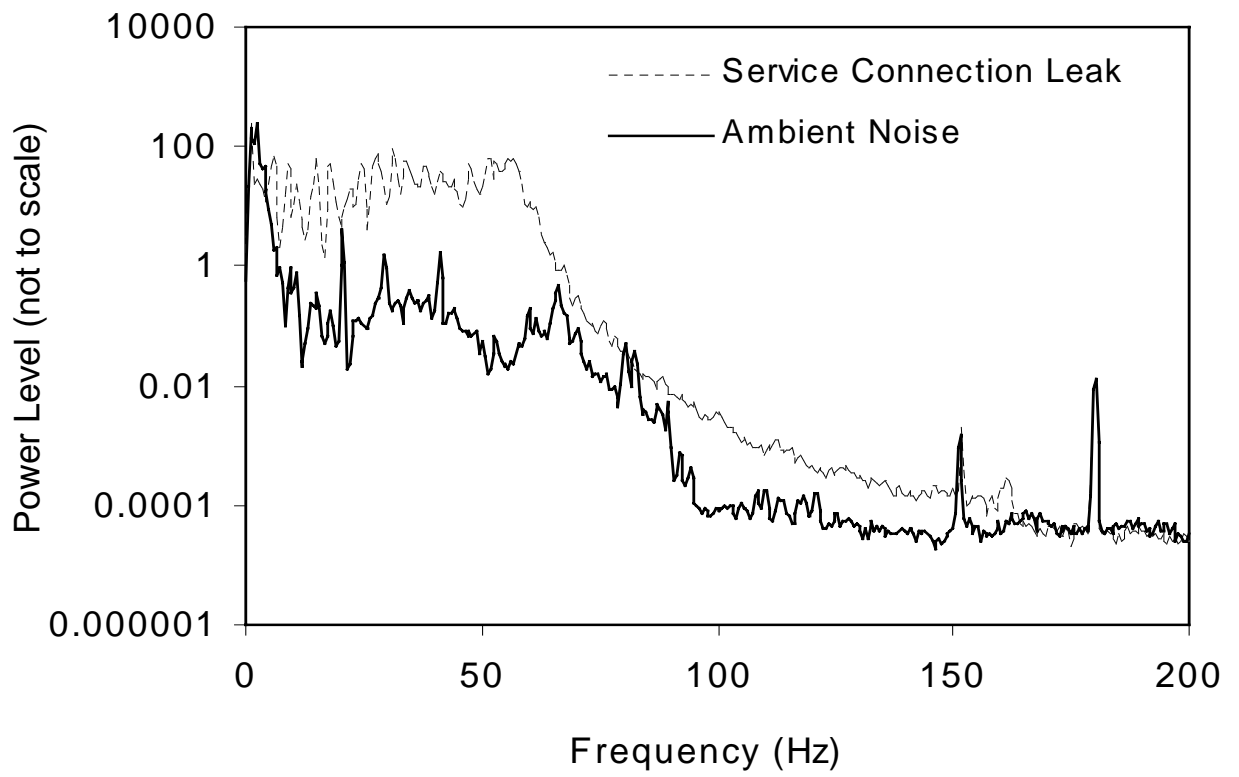


Figure 8a

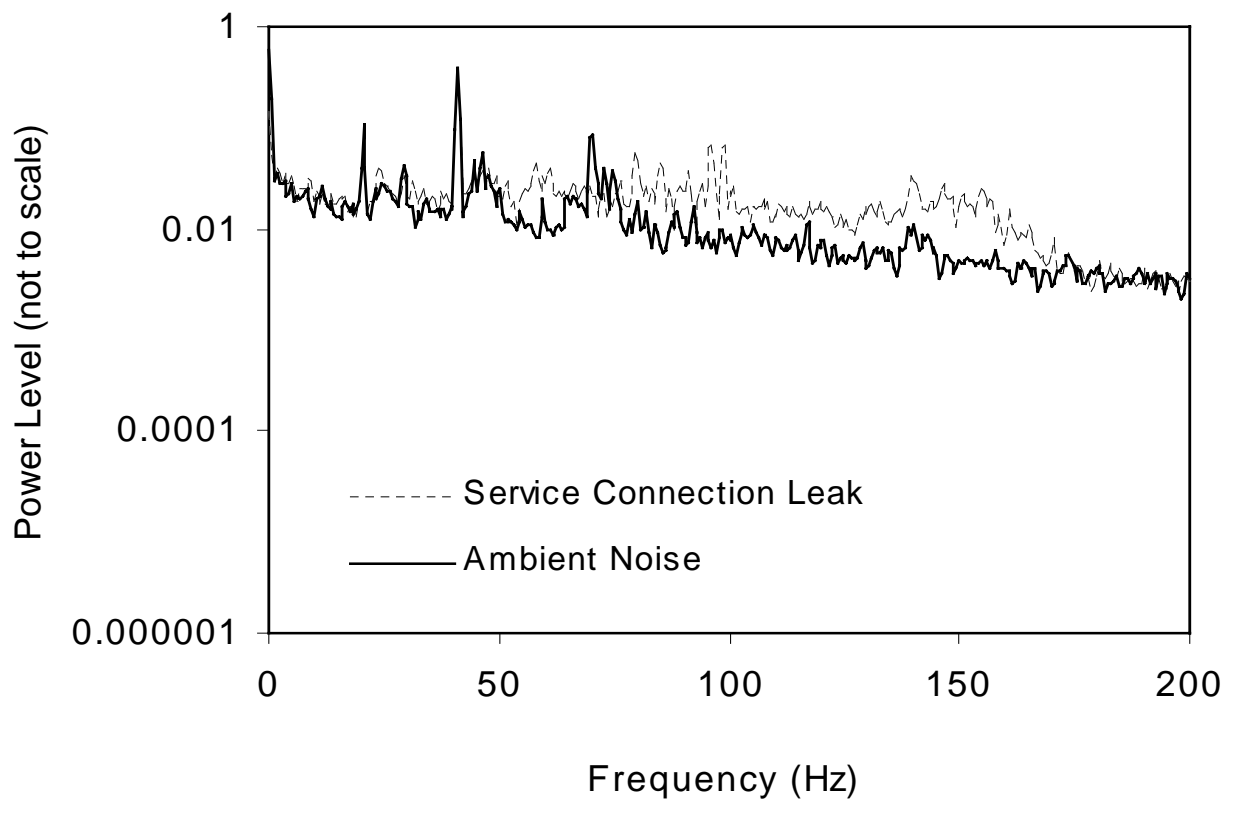


Figure 8b

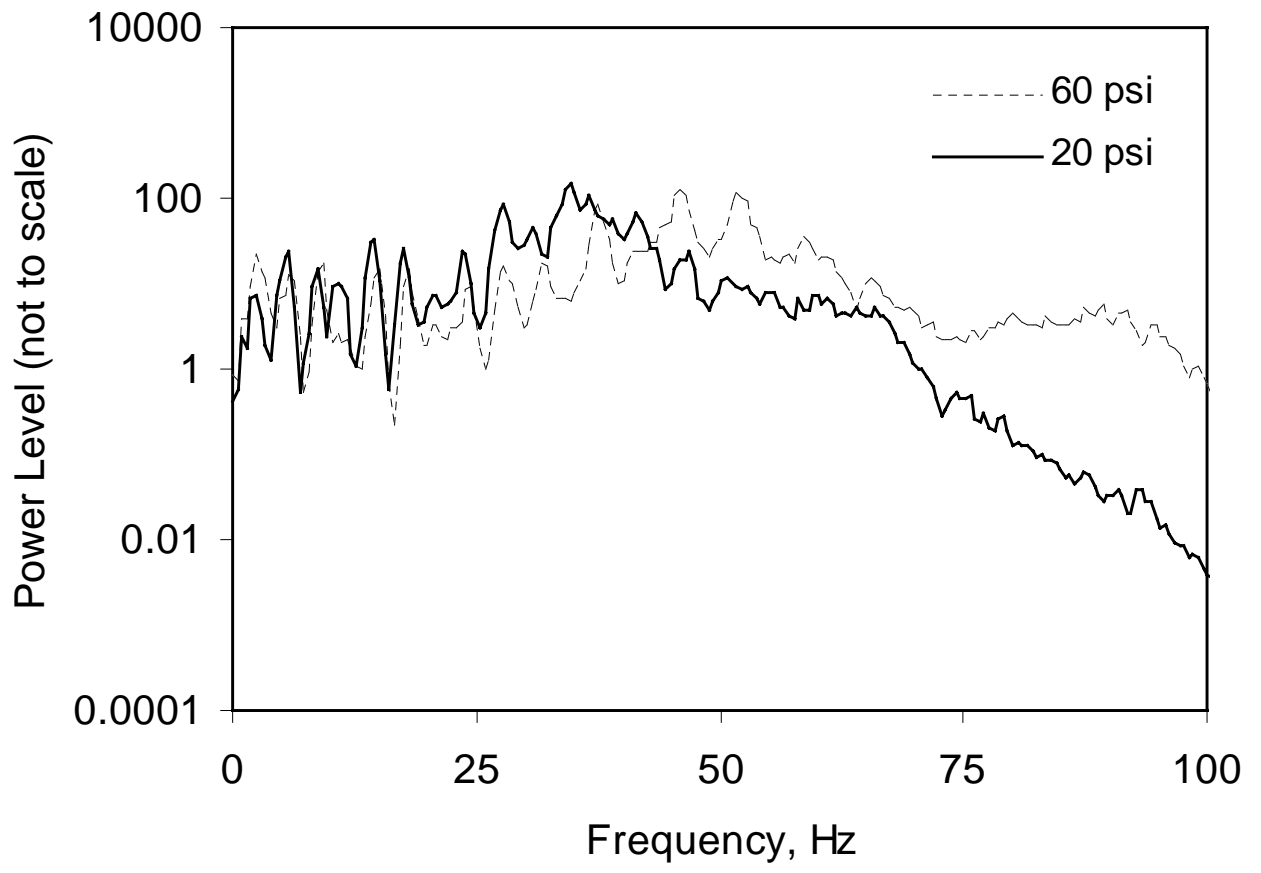


Figure 9

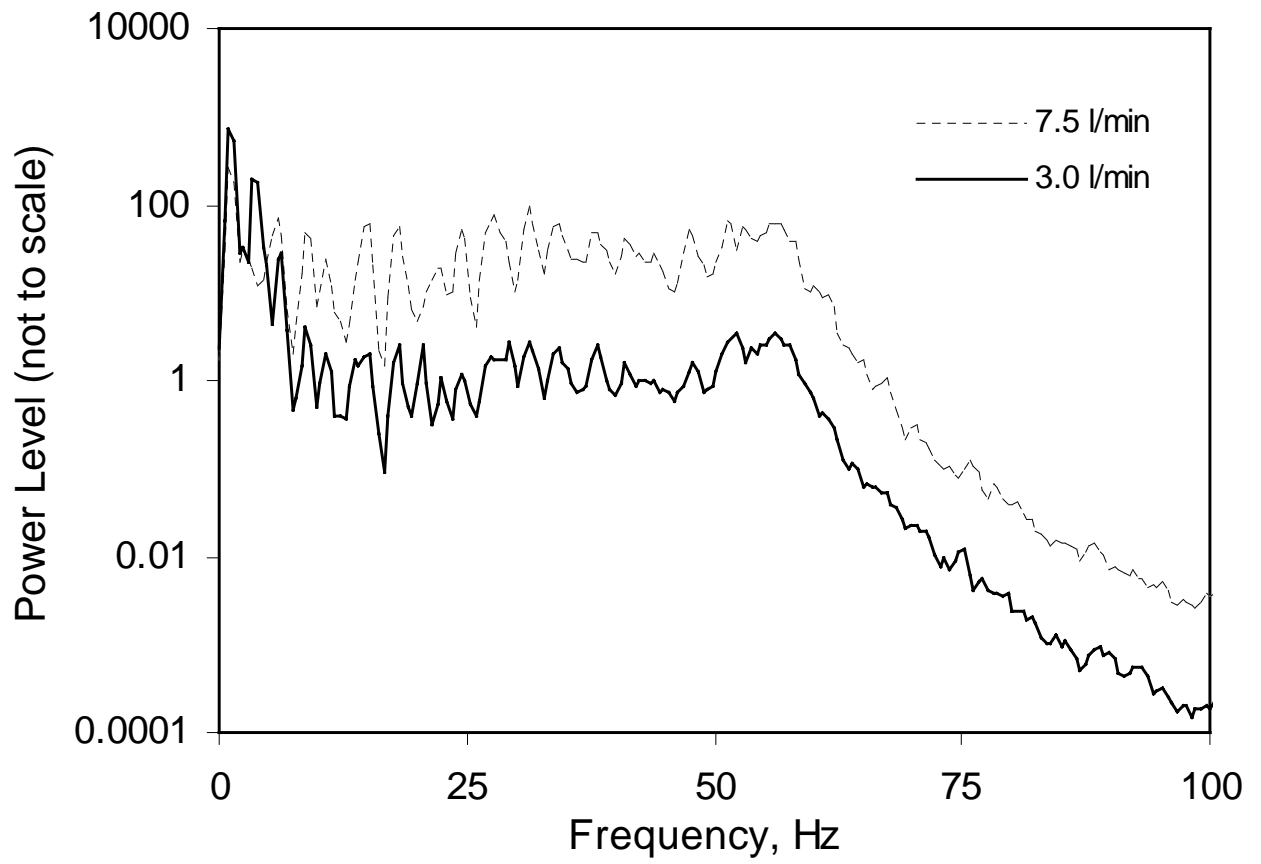


Figure 10

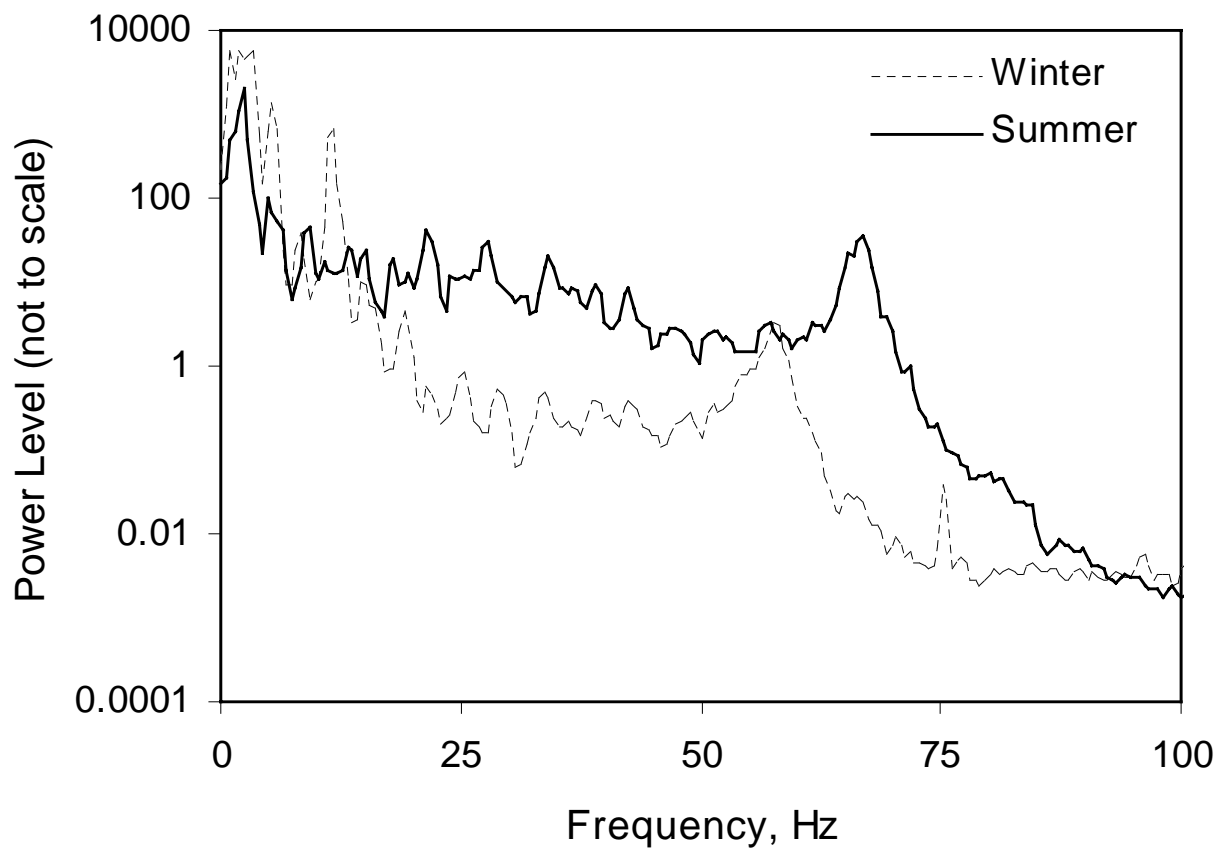


Figure 11

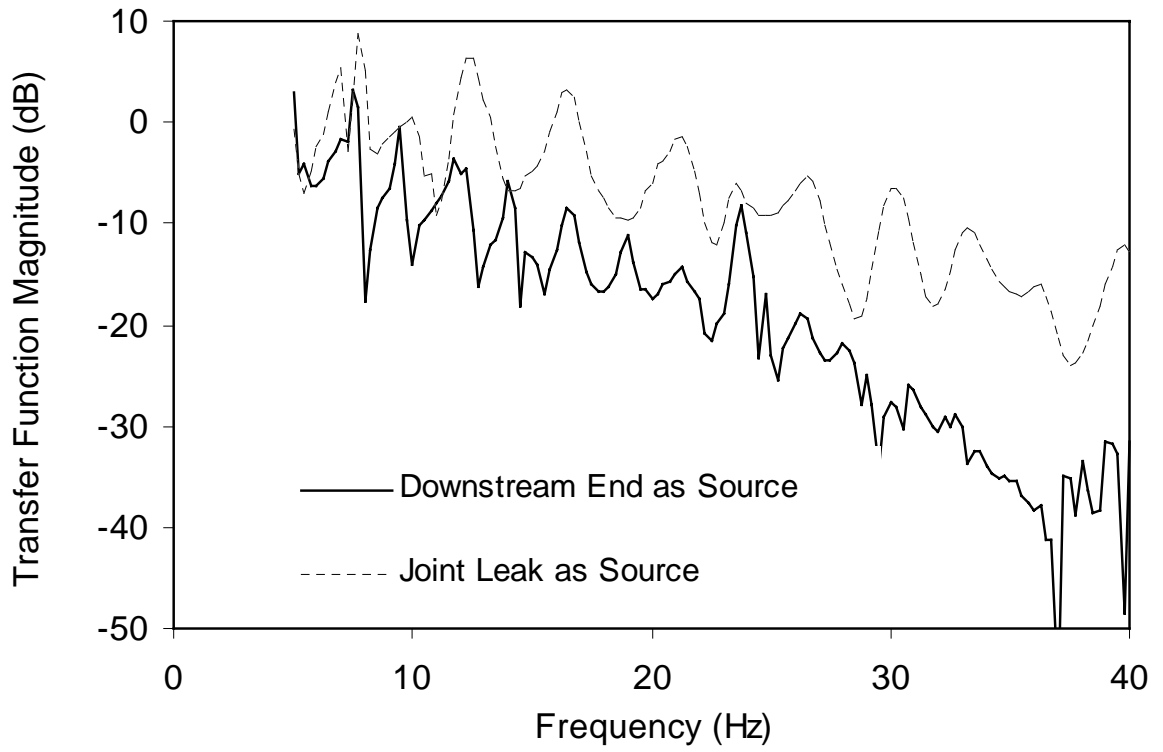


Figure 12

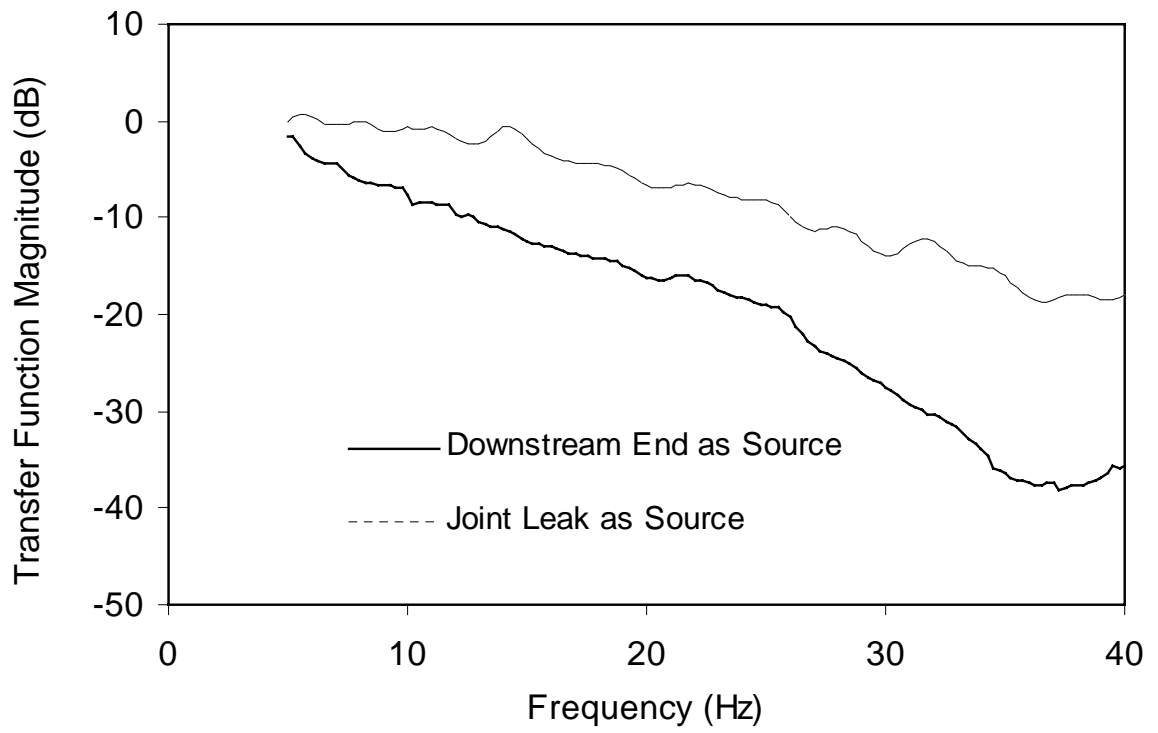


Figure 13

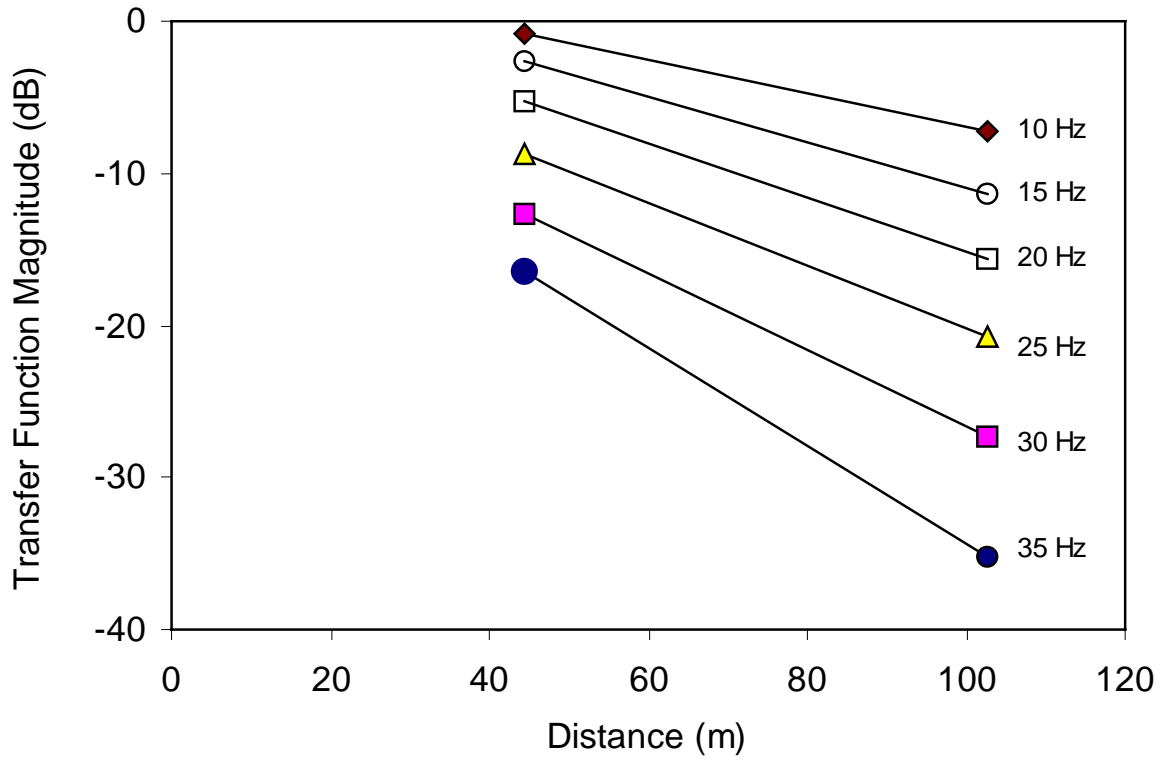


Figure 14

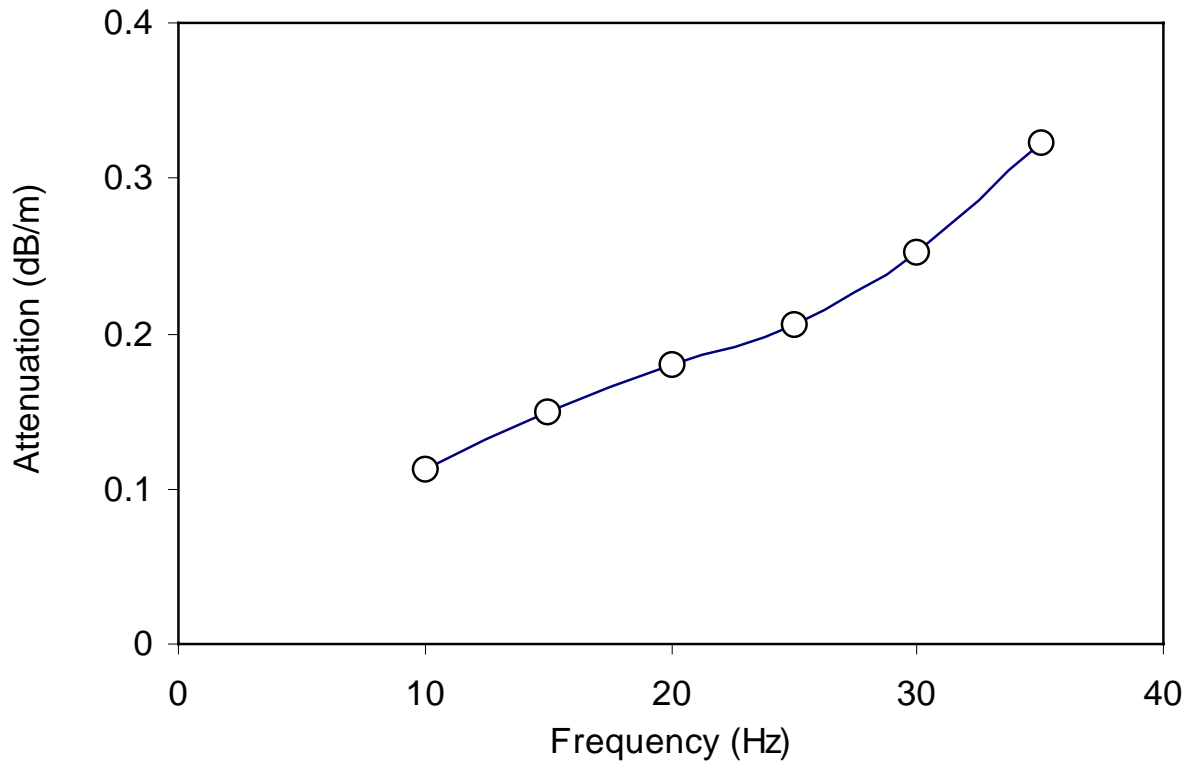


Figure 15

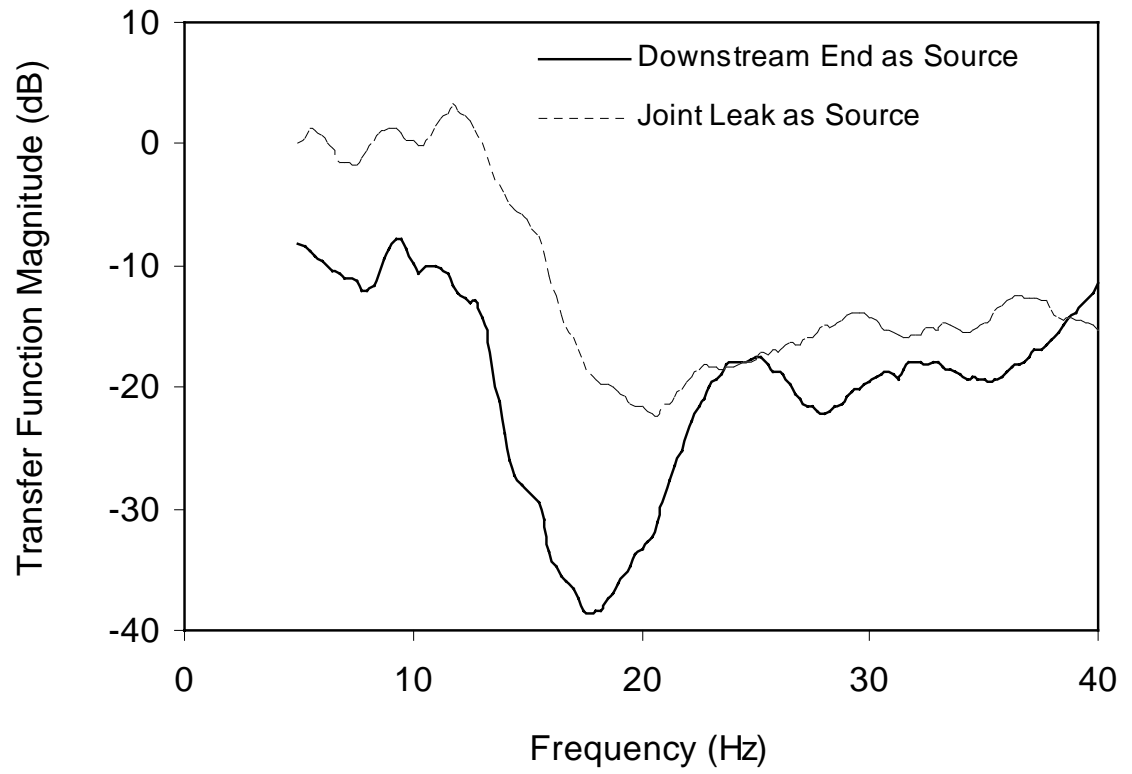


Figure 16

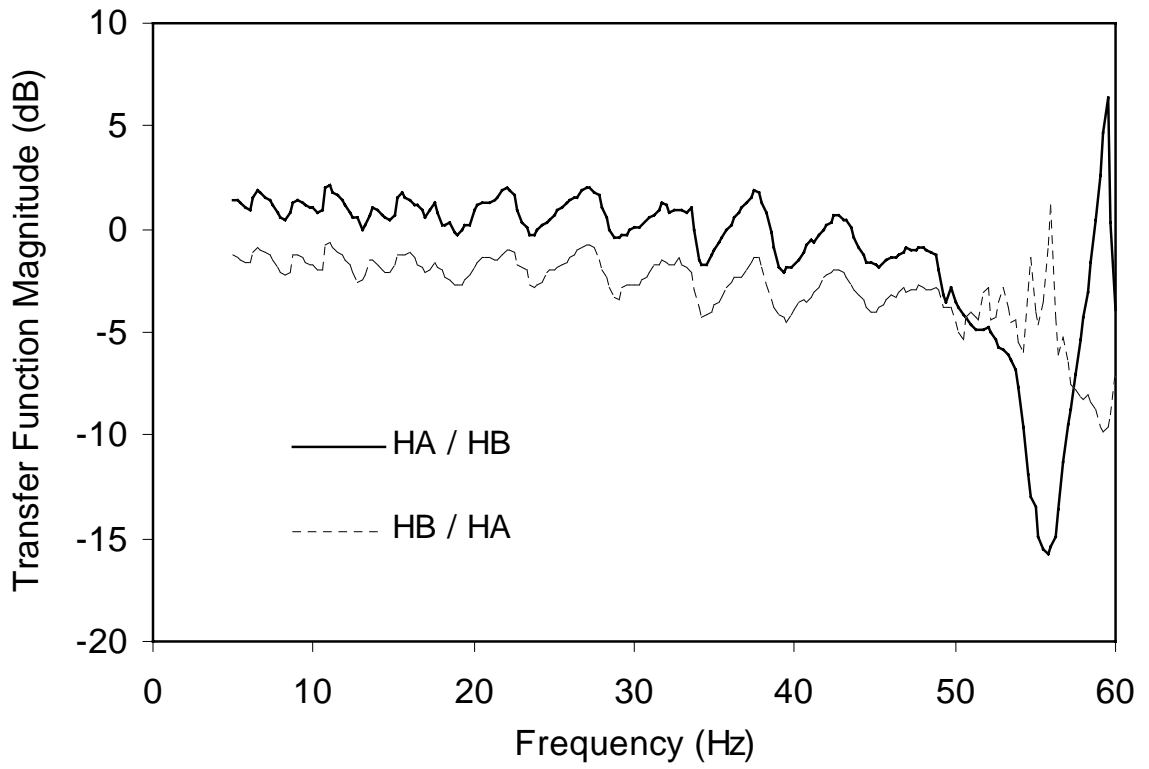


Figure 17

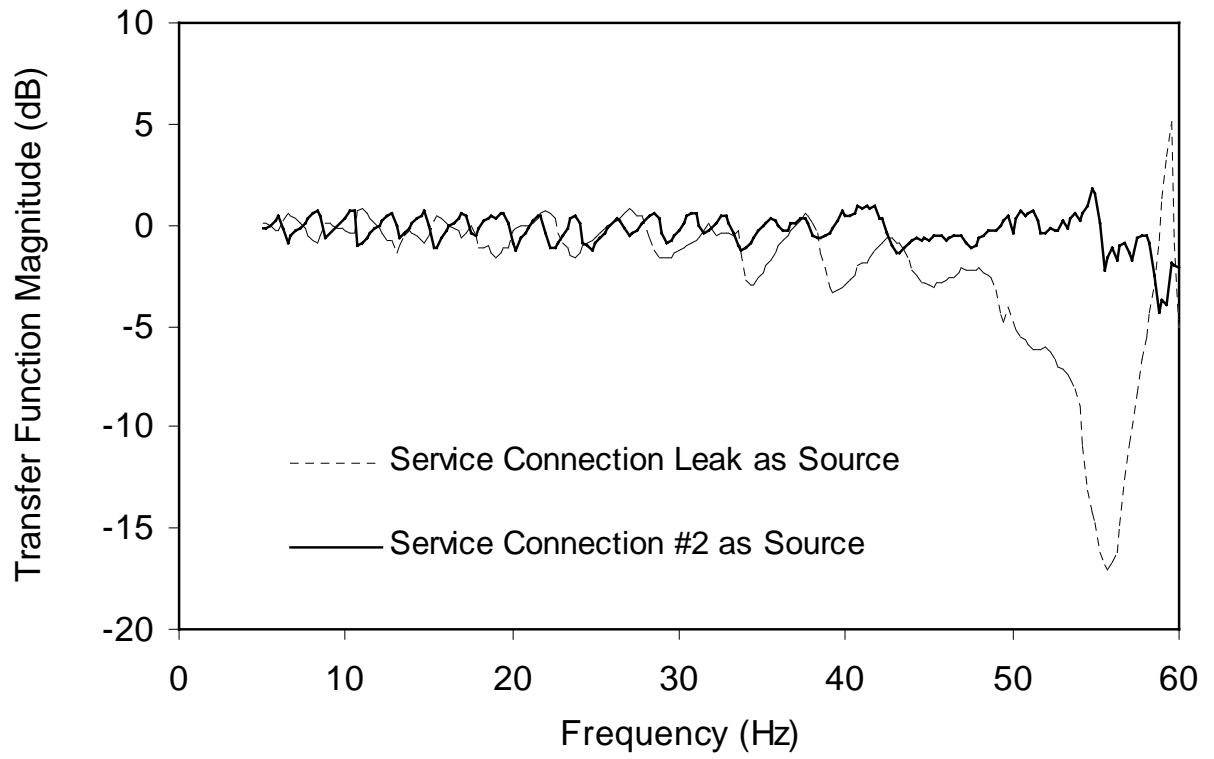


Figure 18

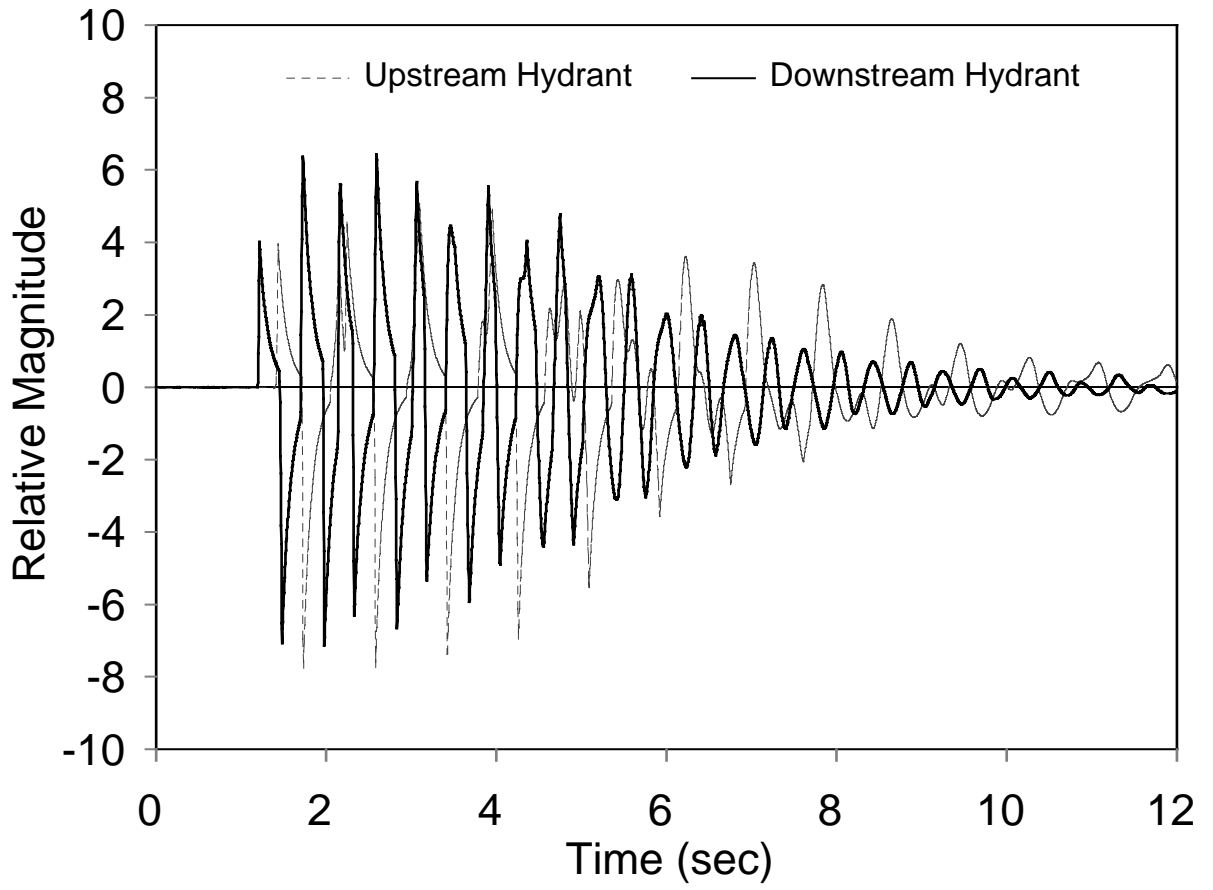


Figure 19

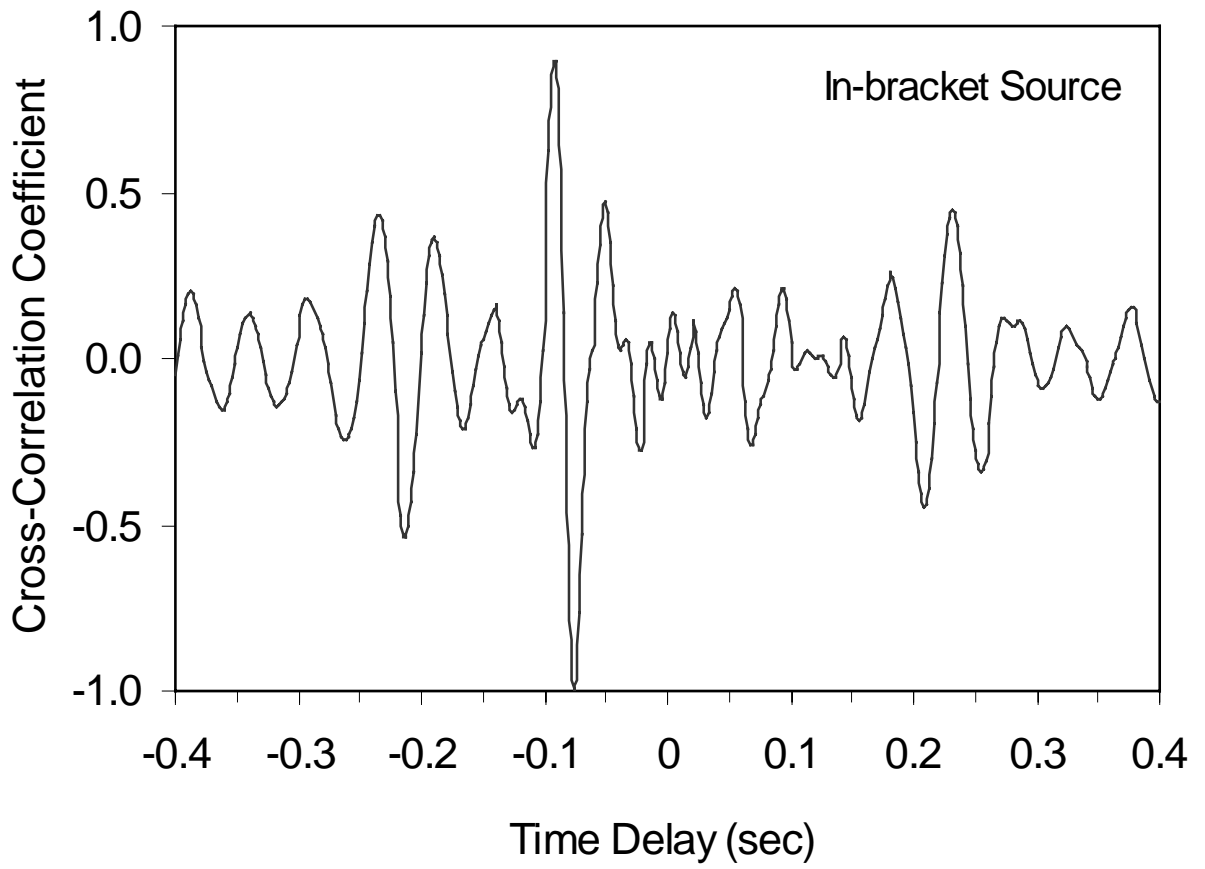


Figure 20a

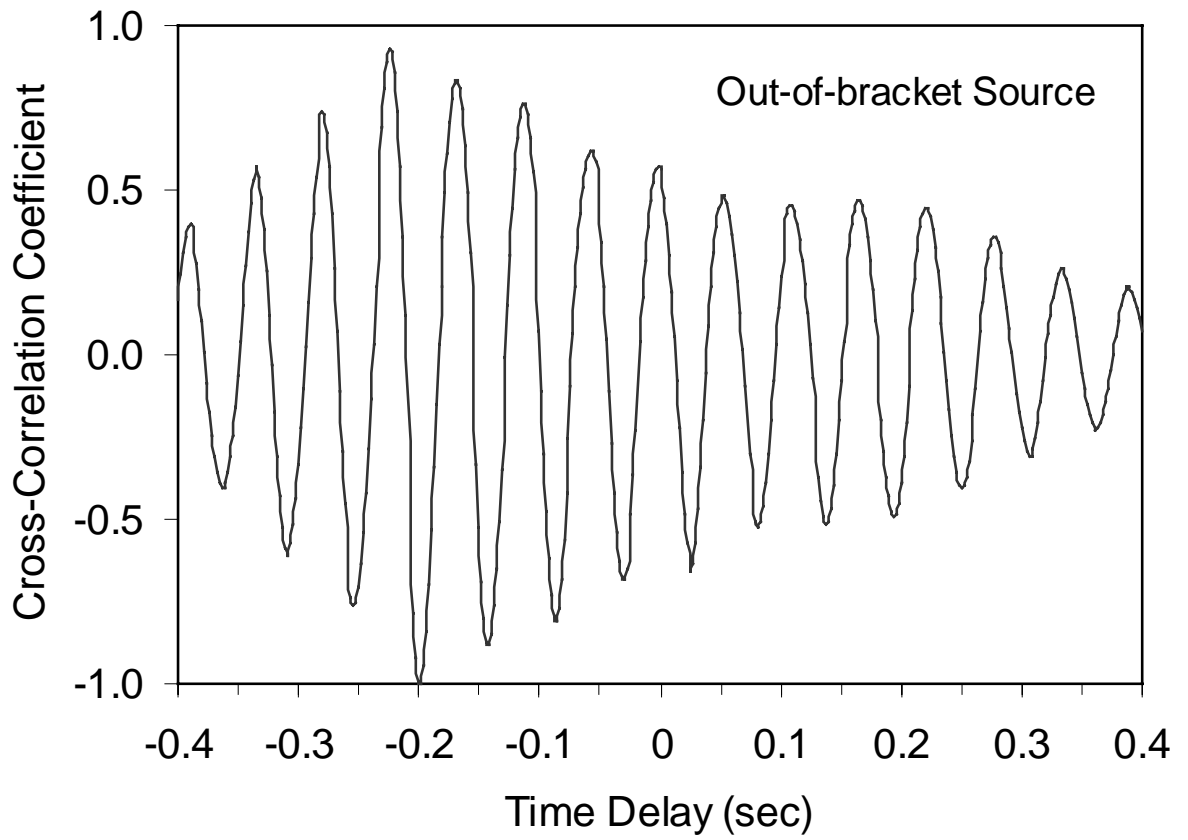


Figure 20b

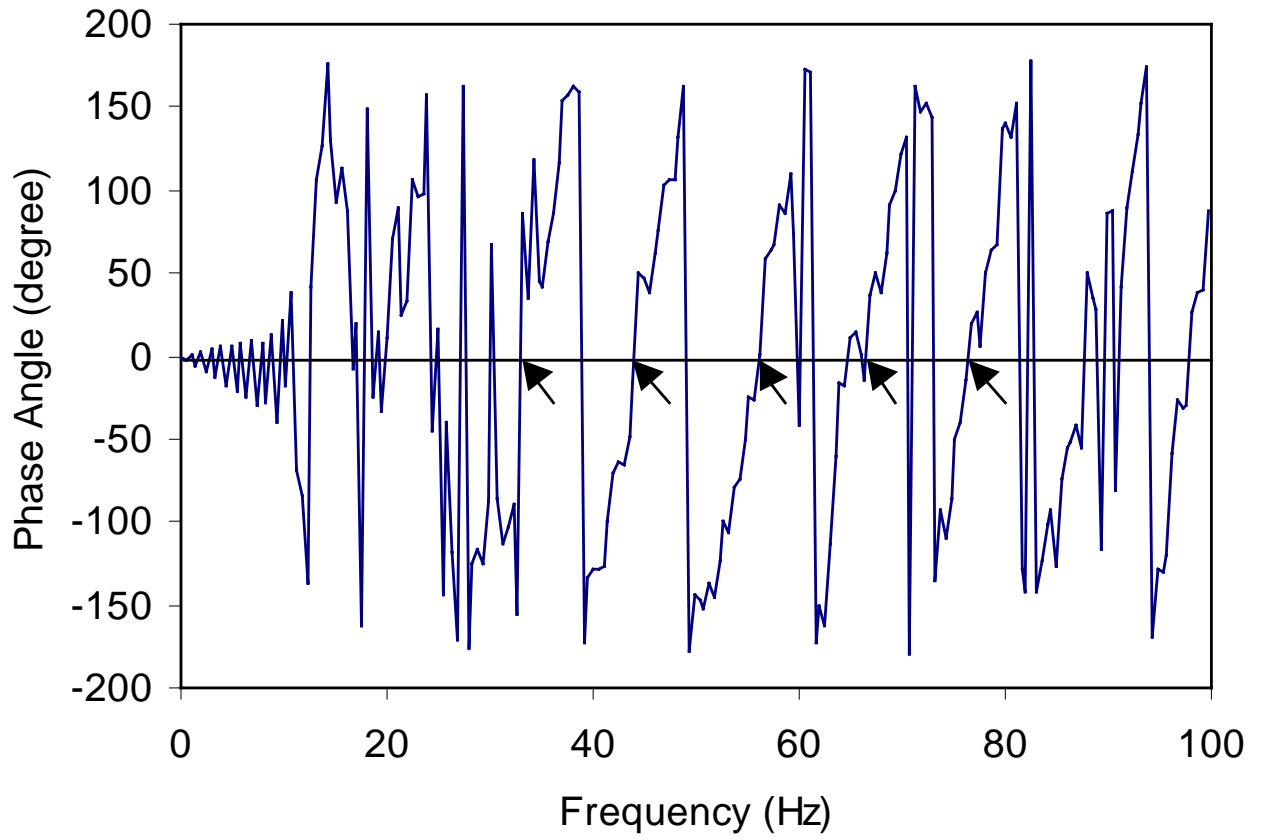


Figure 21

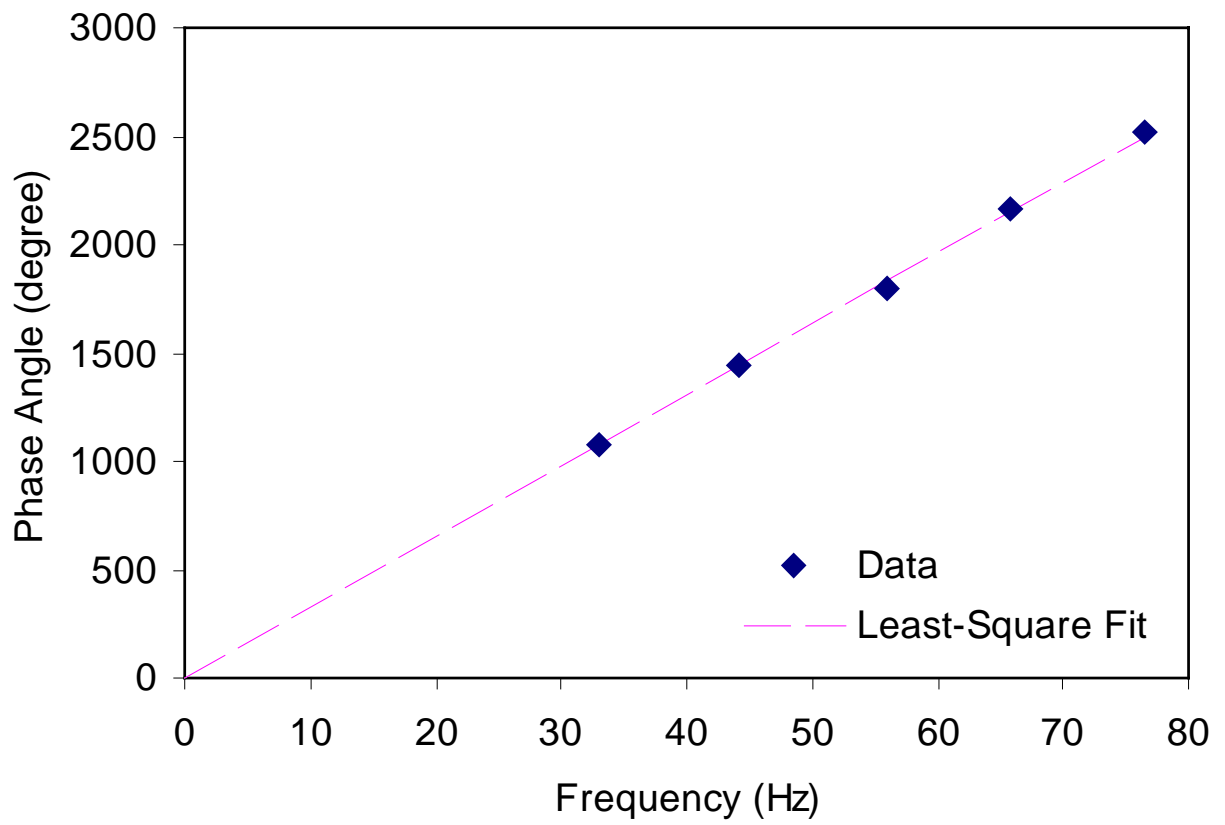


Figure 22